

Mercury Detection using LED techniques:
a feasibility study

Josefin Reftlér
Bachelor Project

Performed at the Division of Atomic Physics
-The Applied Molecular Spectroscopy and Remote Sensing Group
Supervisor: Gabriel Somesfalean

August 28, 2012
Last revised: November 20 2012



LUND UNIVERSITY

Abstract

Mercury is a heavy metal and its presence in our environment constitutes a health-hazard for example in the form of methyl-mercury. Therefore, it is important to construct sensors to detect this pollutant. Research is also being performed on developing optical sensors and mercury can be detected through a range of methods, from point monitoring using Zeeman absorption to 3-D scanning of the atmosphere utilizing Lidar. The aim of the present investigation is to evaluate if a LED in the wavelength region 250-265 nm can be used in order to measure the concentration of the mercury vapour in the air via the 253.7 nm spectral line. This could be used in developing a new type of robust and simple sensor to detect mercury. The theory part of this thesis gives a general introduction to atoms and how they behave, in order to explain the behaviour of mercury. The physics behind the investigation is briefly discussed in order to explain the methods used and developed. The difficulties behind utilizing the LED as a light source is discussed and a comparison with another light source (Hg-lamp) is performed in order to illustrate the differences and challenges between the two light sources. The different designs, which have been developed in an iterative process, are discussed and their performance is compared with each other to describe the process behind the development of the set-ups. Finally the results are presented and discussed. Even though the mercury could not be detected, this investigation lays the foundation for future reference. LEDs will achieve better performance in the future, and we expect this experiment to become more facile, but still not trivial, to perform.

Kvicksilvermätning med LED teknik: en genomförbarhetsanalys

Kvicksilver, Hg, är ett farligt grundämne i miljön då Hg är ett flyktigt ämne. Hg blir farligt för oss människor om det ansamlas i kroppen i form av metylkvicksilver och kan orsaka skador på nervsystemet, njurar och fortplantningsorgan mm. Kvicksilver förs in i vår närmsta livsmiljö i allt större omfattning genom industriprocesser; vanligast är då förbränning av kol och användning i lampor, vulkanisk aktivitet mm. Därför vore det fördelaktigt att ha en kvicksilverfri sensor för att undersöka kvicksilverhalten i luft.

Hur atomen beter sig när den växelverkar med ett elektromagnetiskt fält (t.ex ljus) utgör grunden för denna undersökning. Atomer har olika energinivåer; då ljus av en energi som motsvarar energiskillnaden (bland andra kriterier) mellan två nivåer växelverkar med atomen exciteras atomen och ljusintensiteten blir svagare. Kvicksilver är ett väl undersökt grundämne och metoder som Zeemanabsorption och Lidar kan användas för att undersöka kvicksilverhalten i atmosfären. Det som skiljer denna undersökning från andra är valet av ljuskälla, vilken är en lysdiod, LED, i våglängdsområdet 250-265 nm. Syftet med undersökningen är att se om det går att använda denna sort av ljuskälla för att indikera förekomst av och i förekommande fall utföra undersökningar på kvicksilver.

Arbetet består av två delar, där den svåra delen är att finna en metod för att hitta absorptionsbandet hos kvicksilver. Om absorptionsbandet hittas kommer den andra delen att kunna utföras, vilket är koncentrationsmätningar av kvicksilver vid olika temperaturer. Utrustningen i ett nivåkorsningsexperiment kommer att användas för att göra koncentrationsmätningar, för att en jämförelse mellan ljuskällorna ska kunna göras. Ljuskällan i nivåkorsningen är en kvicksilver lampa, som emitterar starkt vid en välbestämd våglängd, 253.7 nm, till skillnad från dioden som emitterar i ett intervall av våglängder.

Metoden för denna undersökning var inte sammansatt förut och behövde skapas men en initial plan fanns. När de första stegen utfördes av planen sågs vad som fungerade och inte fungerade trots att det borde ha varit optimalt från början. Att samla ljuset från LEDn gav en starkare signal, men begränsade upplösningen av ljuset. Tanken bakom undersökningen var att använda en PMT för att leta efter absorptionsbandet, samt att använda PMTn för att mäta intensitetsskillnaderna då koncentrationen ändras i cellen. Men det som utfördes var att göra detta med en spektrometer, då det är enklare att finna absorptionsbandet med en spektrometer. Det var svårt att erhålla en bra upplösning så att en signal kunde detekteras, då den optiska fibern som samlar ljuset ger denna begränsning. Denna undersökning lägger dock grunden för framtida forskning inom ämnet. I framtiden kommer LED-tekniken att utvecklas och då kommer denna undersökning att kunna förbättras och vara enklare att genomföra.

Contents

Abstract	i
Kvicksilvermätning med LED teknik: en genomförbarhetsanalys	ii
Contents	iii
1 Background	1
2 Theory	2
2.1 The Atom	2
2.1.1 Atomic structure	2
2.1.2 One-electron systems	4
2.1.3 Two-electron systems	7
2.1.4 Many-electron systems	9
2.1.5 Nuclear perturbation	11
2.2 Optical spectroscopy	12
2.2.1 Light sources	13
2.2.2 Optical resolution	15
2.2.3 Grating spectrometers	15
2.2.4 The Beer-Lambert law	15
2.2.5 Detectors	16
2.3 Atomic Spectra	17
2.3.1 One-electron systems	17
2.3.2 Two-electron systems	18
2.3.3 Complex systems	18
2.4 Conclusion	19
2.5 LED (<i>Light emitting diode</i>)	20
3 Method	22
3.1 Instruments	22
3.2 Fluorescence detection of Hg using level crossing spectroscopy set-up	24
3.3 Investigation using a LED source for absorption measurements	25
3.3.1 Method 1	25
3.3.2 Method 2	26
3.3.3 Experiment	28
3.4 Table of contents	29
4 Results	30
4.1 Fluorescence detection	30
4.2 LED absorption measurements	31
5 Evaluation and Discussion	32
6 Appendix	33
6.1 Appendix A	33
7 References	34
8 Bibliography	36

1 Background

Mercury is a poisonous element when accumulated in tissue, since it can inflict damage on the nervous system in humans and animals. Since mercury is a heavy metal it can damage the body in the same manner as other heavy metals do, the heart, kidneys and the reproductive system, amongst other bodily functions [9, 11]. Mercury in the form of methyl-mercury is more dangerous because it can spread from mother to child during pregnancy and pass the blood-brain barrier in humans. [9] Mercury is widely used in industry and is released into the atmosphere through different processes, for example via the incineration of coal. It has been demonstrated that the spread of mercury in the environment is geographically limited by the source [9]

Mercury is used in new energy efficient light sources, which are present in homes, industries and laboratories all over the globe. With the marginalization of incandescent bulbs within EU [13] the use of mercury in light sources increases. Due to the development today, where mercury is used in increasingly many of our personal products it is extremely important to monitor its distribution.

The atomic structure of mercury makes it a very volatile element. This is because it will not react with other elements easily and due to this agglomerates in the environment when once released. Ionised mercury can combine with carbon and hydrogen to produce methyl-mercury. Due to its volatile behaviour, mercury can dissipate over fairly long distances in the atmosphere. [9]

Mercury has a low melting temperature and is the only metal in liquid form at room temperature. Due to this it has a very high vapour pressure at room temperature. This implies that even just a small amount of liquid mercury will fill a room with vapour.

Due to the dangerous effects mercury has on the human body it would be important to develop a detector for investigating the mercury content in closed environments or the free atmosphere. Extensive work on these types of sensors has been performed, and the absorption band of mercury at 254 nm has been mainly investigated [1], however never using a LED (light emitting diode) as a light source.

The mercury content in air has been investigated through methods such as sum-frequency generation with tunable diode lasers [7], Zeeman absorption [5, 14], differential optical absorption spectroscopy (DOAS) [3, 16] and through Lidar techniques [4]. However the sum-frequency generation has the disadvantage that the power of the light is too low for long path monitoring of the concentration of mercury [7]. Research on continuous emission monitors (CEMs) is also being performed with the aim of use at factories and coal plants in order to monitor the actual release of mercury into the atmosphere. [1, 12]

This thesis will first discuss the general theory of the atom, not only mercury, to provide the reader with the basic insight needed to understand the spectral behaviour of atoms. It also has the intent of being a sum up of the atomic physics a bachelor student should know.

Briefly, the physics behind some of the methods concerning spectral resolution is discussed. This structure is chosen in order to give an overview of the basic physics behind the different components of this investigation.

The intention with this study is to evaluate if mercury concentration measurements can be performed using a broadband light source, as an LED.

This investigation consists of three parts which will be treated consecutively. The first step is to find the absorption band and if this is achieved the intention is to perform a series of concentration measurements of mercury at different temperatures. The primary purpose

of the investigation is to explore if such measurements can be performed with a LED as a light source. The third part is to compare the LED measurements with concentration measurement using another light source. The equipment in the level crossing spectroscopy lab exercise is used in order envisage the fluorescence intensity variation with temperature of the mercury cell. The light source for excitation is a mercury lamp, which provides a perfect fit for absorption measurements.

2 Theory

In this part the atom will be presented both classically and quantum- mechanically in order to explain the general behaviour of the atom. The chapter will start with a short summary of the atom - both the electronic and nuclear structures - then the primary factor behind the behaviour of the atom- the electron systems- will be discussed. This will be used in order to explain the spectra that are received from different atoms. This is done to present the complexity about atoms and atomic spectroscopy. Some of the instruments that can be used for optical spectroscopy will be briefly discussed in order to give a picture on their functions and how spectral resolution can be achieved. Thereafter, the interpretation of the results and the relevance of the experiment will be explained. The light source of this investigation will be shortly described, and some of the concepts in solid state physics will be presented briefly to give some background about LEDs.

2.1 The Atom

2.1.1 Atomic structure

The most basic thing about the atom is that it consists of three types of particles, protons, neutrons and electrons, and of two types of structures. The atom consists of a nucleus, where protons and neutrons are located and around it there are electrons in well defined orbits which correspond to the energy levels of the atom. The number of protons give which element the atom belongs to, as this is what separates an element from another and the number of neutrons give which isotope of the that element it belongs to. The proton has one positive unit charge and the electron has one negative. The atom as a whole should be electrically neutral, so the electron density give whether the element is neutral or an ion. The physical and chemical properties of the atom are mainly due to the electron structure of the atom, and whether or not the atom is neutral as the Coloumb potential stays the same; however, if the electron charge density increases or decreases, the electrons will be subject to less or more than one unit charge from the nucleus and as a result will be less or more tightly bound by the nucleus' field.

Electronic structure The electron structure corresponds to certain energy levels in the atom, and their location is governed by a set of quantum numbers. The energy levels are never the same for different elements as the atomic environment changes when the number of protons varies as this alters the Coulombic potential which the electrons feel. The chemical and physical properties, such as ionization energies and place in the periodic table can be explained shortly by the electron structure.

The electrons have a set of quantum numbers with the principal quantum number n which can be read as a principal contribution to the energy level which the electron is situated in. The others are l which determines the angular momentum of the electron and constitutes the orbital of the energy level and another quantum number m_l which dictates the projection of the orbital angular momentum onto a direction in space. The

quantum number s is the spin quantum number to which m_s belongs yielding the direction of the electron spin projection, that is spin up or down. These are the rules about how the electrons may place themselves in the orbitals and energy levels, called shell theory. The electrons place themselves in shells obeying the Pauli principle (that no two fermions with the same quantum number can share the same state) as will be discussed and shown later; and according to the Aufbau principle (that the electron configuration is most stable if the energy levels are filled with the electrons in a certain way), where the electrons with the same quantum number m_s are placed in the orbital first, with the quantum numbers m_l different, in order so that the lowest possible energy is achieved. This can be depicted in the table below.

l	0	1	2	3	4
$n = 1$	1s				
$n = 2$	2s	2p			
$n = 3$	3s	3p	3d		
$n = 4$	4s	4p	4d	4f	

The electronic shell structure of Neon can be seen in Fig.1 and from this the Aufbau principle as well as the Pauli principle can be envisaged. How the known quantum numbers arose will be explained later, in section 2.1.1.

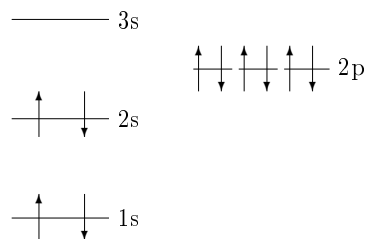


Figure 1: Electronic shell structure of Neon

Nucleon structure Could it be possible that the protons and neutrons themselves form well defined shells as the electrons do? The probability for the nucleons to collide and transfer energy amongst themselves is higher than for the electrons as the electrons are smaller and occupy a larger space. [10] Solving the Schrödinger equation (SE) for the nucleons is a hard task, as the potential which the nucleons feel is different from the Coulombic one, and arises from the interactions amongst the nucleons. [10] However, if the solution of the Schrödinger equation indicates quantum numbers as for the electrons then a shell theory for the nucleons can be constructed; to this it can be argued that if the nucleons indeed collide and transfer energy as a result, this can only occur if the nucleon ends up in a higher energy state that is not already occupied by another nucleon. This would require more energy than is possible to transfer, so this event cannot occur. The nucleons do not collide and can occupy a shell structure. [10] It can even be argued that as the nucleons govern their own potential, this potential makes sure that no nucleons collide. The solution, even though hard to perform, indicates that in contrast to the electronic case, the principal quantum number for the nucleons is the angular momentum l . The protons and the neutrons form their own shells respectively to this, e.q Fig.2.

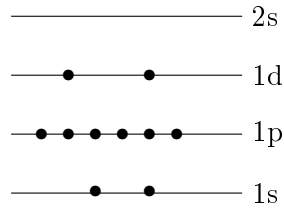


Figure 2: Proton shell structure of Neon

2.1.2 One-electron systems

One-electron systems are atoms which have one valence electron. The most simple one-electron system is the hydrogen atom, which has one proton in its nucleus and one electron in an orbit around it. The SE for this system is the easiest to solve as this system does not have any other interactions than the ones between the proton and the electron. Solving the SE for the Hydrogen atom constitutes a basis for other one-electron systems and, as will be later shown, for two-electron systems as well.

One-electron systems can thus be said to be hydrogen-like systems. The ground state electron is a 1s electron and this electron has a probability to be inside the nucleus due to its spherical symmetry. [2] When solving the SE for the hydrogen atom it has to be decided if the common centre of mass is going to be used or assuming that the nucleus is the center. When using the common centre of mass the *reduced mass*

$$\mu = \frac{m_e M}{m_e + M}$$

is used in the Hamiltonian. The Hamiltonian is the energy operator for which the energy eigenvalues can be found, or in other words, the energy levels of the atom. The time-independent SE is used to calculate the energy levels, as these are stationary, and takes the form

$$H\Psi(\vec{r}) = E\Psi(\vec{r})$$

where H is the Hamiltonian

$$H = \underbrace{\frac{p^2}{2\mu}}_{\text{kinetic energy}} + \underbrace{V(r)}_{\text{potential energy}} = \underbrace{-\hbar^2 \frac{\nabla^2}{2\mu}}_{\frac{p^2}{2\mu}} - \underbrace{\frac{Ze}{4\pi\epsilon_0 r}}_{V(r)}$$

and E is the solution to the Hamiltonian, the eigen-energies to that state. [2] Z is the number of protons in the atom. The potential of the Hamiltonian is spherically symmetric and expressing the Hamiltonian in spherical coordinates, by substituting the ∇^2 with its form in spherical polar coordinates yields

$$\nabla^2 = \frac{1}{r^2} \frac{\partial}{\partial r} \left(r^2 \frac{\partial}{\partial r} \right) + \frac{1}{r^2 + \sin^2 \theta} \frac{\partial}{\partial \theta} \left(\sin^2 \theta \frac{\partial}{\partial \theta} \right) + \frac{1}{r^2 \sin^2 \theta} \frac{\partial^2}{\partial \phi^2}$$

and expressing the eigen-function as such:

$$\Psi(r, \theta, \phi) = R(r)Y(\theta, \phi)$$

[2] The angular part can be further separated into the spherical harmonics, which give the angular distribution of the wavefunction

$$Y_l^m(\theta, \phi) = \Theta(\theta)\Phi(\phi)$$

The SE can be solved for these separated forms and the quantum number m_l and l can be obtained from this. For the complete solution of the SE, see *appendix A*.

Since the angular momentum operator square is known when it acts upon a state

$$\vec{l}^2\Psi(\vec{r}) = l(l+1)\hbar\Psi(\vec{r})$$

the magnitude of the angular momentum of the electron can be obtained, $\sqrt{l(l+1)}\hbar$. The component of this in the z -direction is $m_l\hbar$. The quantum number n results from using what is known and solving the radial part of the Schrödinger equation. The energy eigen-values, hence the solution of the Schrödinger equation becomes (non-relativistic wave-function)

$$E_n = -\frac{1}{2} \frac{e^4\mu}{(4\pi\epsilon_0)} \frac{Z^2}{n^2} \equiv -R_M \frac{Z^2}{n^2}$$

where R_M is the Rydberg's constant for which the reduced mass has been used. The correspondence between the Rydberg constant where the reduced mass has been used and the fictitious case when the center of mass coincides with the position of the nucleus is

$$R_M = R_\infty \frac{\mu}{m_e} = R_\infty \frac{M}{M + m_e}$$

[2] The principal quantum number n can have positive integer values ranging from one to infinity. The l quantum number takes integer values from 0 to $n-1$, and has this restriction because it is connected to both the radial *and* angular part of the wave-function. The states $l = 0, 1, 2, 3, 5\dots$ are called s,p,d,f,g,h... so in an energy diagram (see fig 1); this is what the notation means. The quantum number m_l take integer values $-l \leq m_l \leq l$. [2] The wave-function can be written

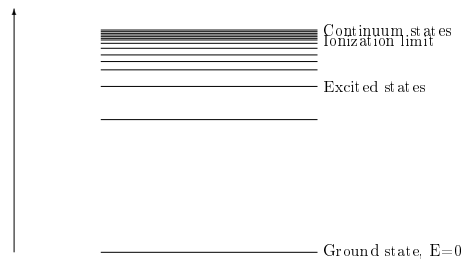
$$\psi_{nlm}(r, \theta, \phi) = R_{nl}(r)Y_l^m(\theta, \phi)$$

The parity of the wave-function is governed by l ; the parity reverses the position of the state. The parity of the wave-function and the wave-function itself is even when l is even, and vice versa. [2] The probability to find the electron in a given volume element is given by the absolute square of the wave-function in the given volume.

$$|\psi(r, \theta, \phi)|^2 dV$$

[2]

Knowing this the energy level diagram for the Hydrogen atom could look like e.g.



[2]

The spin quantum number was introduced in order to explain the fine structure that arises when an energy level splits in the presence of an applied magnetic field, the so called *Zeeman effect*. The outcome of the *Stern-Gerlach* experiment provided evidence for the spin s and the quantum number m_s .

The fine structure of the energy levels arises from the magnetic moment which is coupled to the spin, as the spin can be thought as the angular momentum of the rotation of a charged body which in this case is the electron. The magnetic moment μ_s becomes, if relativistic effects have been accounted for,

$$\vec{\mu}_s = -g_s \frac{e}{2m_e} \vec{s}$$

where \vec{s} is the spin angular momentum vector and g_s is called the gyromagnetic ratio [2], and has a value of approximately 2. The magnetic moment will then have a component in the direction of the magnetic field (the z -direction) which depends on the strength of the magnetic field

$$(\vec{\mu}_s)_z = -g_s \frac{e\hbar}{2m_e} m_s = -g_s \mu_B m_s$$

[2] The fine structure corresponds to the field created by the electronic motion that couples to the angular momentum of the electron, which is called the spin-orbit interaction [2]. The potential energy of the electron, in the magnetic field which is created due to this motion, is

$$E_{so} = -\vec{\mu}_s \cdot \vec{B}_l = C \cdot \vec{l} \cdot \vec{s}$$

where C is a proportionality constant which is known for the one-electron case (however becomes more difficult to find for many electrons). The energy will depend on the scalar product between the angular momentum and spin. Defining a property called the total angular momentum \vec{j} of the electron, which is the sum of the angular momentum and the spin of one electron.

$$\vec{j} = \vec{l} + \vec{s}$$

The quadrated term of the total angular momentum facilitates the expression for the spin-orbit energy as the scalar product can be expressed in simpler terms.

$$\vec{j}^2 = \vec{l}^2 + \vec{s}^2 + 2\vec{l} \cdot \vec{s} \Leftrightarrow \vec{l} \cdot \vec{s} = \frac{1}{2} (\vec{j}^2 - \vec{l}^2 - \vec{s}^2)$$

Now the result can be found, using what the quantum operators give when acted upon a state. [2]

$$\begin{cases} \vec{j}^2 |j, m_j, l, m_l\rangle = \hbar^2 j(j+1) |j, m_j, l, m_l\rangle \\ \vec{l}^2 |j, m_j, l, m_l\rangle = \hbar^2 l(l+1) |j, m_j, l, m_l\rangle \\ \vec{s}^2 |j, m_j, l, m_l\rangle = \hbar^2 s(s+1) |j, m_j, l, m_l\rangle \end{cases}$$

Dirac notation has been used in order to express the electronic state, as it facilitates to see how the operators acts on the state. The Dirac notation for our state before the total angular momentum was introduced was $|n, l, m_l, s, m_s\rangle_1$ and becomes with angular momenta a composite state $|j, m_j, l, m_l\rangle_2$; which is a linear combination of state one, where the coefficients of this linear combination are called the *Clebsch-Gordon* coefficients. The new quantum number j is the total angular momentum and the component of this in z -direction is the quantum number m_j , which takes the values $-j \leq m_j \leq j$. [2] When using the received eigenvalues the potential energy thus becomes,

$$E_{so} = C \vec{l} \cdot \vec{s} = \frac{1}{2} (\vec{j}^2 - \vec{l}^2 - \vec{s}^2) = \hbar^2 C (j(j+1) - l(l+1) - s(s+1))$$

When taking the fine structure effect into account, it becomes evident that the energy level depends on the quantum numbers j and n , but not on l or m_j . [2]

2.1.3 Two-electron systems

In analogy to one-electron systems, two electron systems are atoms which have two valence electrons, and these atoms are called Helium-like atoms [2] of charge Ze^2 (where Z is the number of protons). However, the Hamiltonian now contains an additional term due to the electrostatic repulsion the electrons exert on each other. Hence the Hamiltonian takes the form (when infinitely heavy nucleus is assumed),

$$H = \underbrace{-\frac{p_1^2}{2m_1} - \frac{p_2^2}{2m_2}}_{\text{kinetic energy}} - \underbrace{\frac{Ze^2}{4\pi\epsilon_0 r_1} - \frac{Ze^2}{4\pi\epsilon_0 r_2}}_{\text{pot. energy}} + \underbrace{\frac{e^2}{4\pi\epsilon_0 r_{12}}}_{\text{electrostatic repulsion pot. energy}}$$

The $r_{ij} = |\vec{r}_i - \vec{r}_j|$, where $i = 1$ and $j = 2$, is the distance between the two electrons. Solving the stationary SE with this Hamiltonian becomes a more difficult task, and as this problem corresponds to the classical three-body problem and no three-body problems can be solved. This implies that the Schrödinger equation cannot be solved exactly. The first step to solve it will be to omit the most difficult term, the electrostatic repulsion. The remainder will be easier to handle as this can be separated into two equations and due to the fact that the particles are identical they will both have the same solution. The result of these two equations will be two one-electron wave-functions and the final wave-function will be the product of these. [2]

$$\psi_{a,b}(\vec{r}_1, \vec{r}_2) = \psi_a(\vec{r}_1) \cdot \psi_b(\vec{r}_2)$$

The indices a and b in the wavefunction "represent the quantum numbers n, l, m_l of each electron"¹. The energy eigen-values for each of the separated equations will be of hydrogenic form so the total energy eigenvalue will be the sum of these

$$E = \epsilon_1 + \epsilon_2 = -RZ^2 \left[\frac{1}{n_1^2} + \frac{1}{n_2^2} \right]$$

As the particles are identical the eigenvalue will remain the same when the electrons are exchanged.

However, it is not always true that the wave-function remains unchanged if the order of the two particles are changed, and as the probability has to be unchanged:

$$|\psi_{a,b}(1, 2)|^2 = |\psi_{b,a}(1, 2)|^2$$

Linear combinations of the hydrogenic wave-functions can be constructed that fulfil the probability requirement.

$$\begin{aligned} +\psi &= \frac{1}{\sqrt{2}}[\psi_{a,b}(1, 2) + \psi_{b,a}(1, 2)] \\ -\psi &= \frac{1}{\sqrt{2}}[\psi_{a,b}(1, 2) - \psi_{b,a}(1, 2)] \end{aligned}$$

These two equations are solutions to the Schrödinger equation where the probability has been taken into account, the first one is symmetric (+) and the other one is antisymmetric (-).

To this point one of the known quantum numbers has been neglected; however the electronic spin has been taken into account due to that it only affects the wave-function as being odd or even. Hence the total wave-function can be constructed. [2]

$$\Psi(1, 2) = \underbrace{\psi(1, 2)}_{\text{space function}} \cdot \underbrace{\chi(1, 2)}_{\text{spin}}$$

¹A. Thorne U. Litzén S. Johansson, *Spectrophysics principles and applications*, 2007, Media Tryck Lund, p27

Still the wave-functions constructed from this need to follow the probability condition. Both symmetric(+) and antisymmetric(-) functions (as before) satisfy this. The knowledge about the fermionic case (spin = $\frac{1}{2}$) for identical particles give evidence for them being antisymmetric total wave-functions. This is the mathematical construct of the Pauli principle as

$$\Psi_{a,b}(1, 2) = -\Psi_{b,a}(1, 2)$$

saying that the wave-function and hence the state does not exist when $\Psi \equiv 0 \rightarrow a \equiv b$. Hence the identical particles of spin $\frac{1}{2}$ cannot have identical quantum numbers.

Considering the projection in z -direction of the spin, to identify the different spin states, give the quantum number $m_s = \pm\frac{1}{2}$, which is read as spin up and spin down. Constructing symmetric and antisymmetric spin parts to the total wave function from this gives

$$\begin{aligned}\chi_1(1, 2) &= \alpha(1)\alpha(2) \\ \chi_2(1, 2) &= \alpha(1)\beta(2) \\ \chi_3(1, 2) &= \beta(1)\alpha(2) \\ \chi_4(1, 2) &= \beta(1)\beta(2)\end{aligned}$$

where α and β give spin up or down respectively. A new quantum number can be constructed from the projection of the total spin, called M_S , which is the sum of the individual m_s , or more easily constructed the sum of the spins, the quantum number S [2]. Hence the functions will have $M_S = 1$, $M_S = 0$, $M_S = 0$ and $M_S = -1$ respectively. From this construct χ_1 and χ_4 will be symmetric functions as nothing would happen if the particles changed place and have $M_S = 1$ and $M_S = -1$ respectively. [2]

χ_2 and χ_3 can be combined to create two new functions, one symmetric and the other antisymmetric

$$\begin{aligned}^+\chi_{23} &= \frac{1}{\sqrt{2}}[\alpha(1)\beta(2) + \beta(1)\alpha(2)] \\ ^-\chi_{23} &= \frac{1}{\sqrt{2}}[\beta(1)\alpha(2) - \alpha(1)\beta(2)]\end{aligned}$$

both with $M_S = 0$. Hence the symmetric states can have three projections of the total spin $S = 1$ as S takes the values $M_S = -1, 0, 1$, while the antisymmetric case only has $M_S = 0$, $S = 0$. These projections are important as spin-orbit interactions take place as well. When the total spin is 0 there will be no fine structure and these will form singlet states. When the total spin is 1 there will be a fine structure as the M_S can take three values and be called triplet states. [2]

The omitted term of the Hamiltonian, the electron interaction, can be treated as a perturbation as the energy levels will deviate from the energy calculated to this point. The omitted term is:

$$H' = \frac{e^2}{4\pi\epsilon_0 r_{12}}$$

The energy contribution with which the energy level will deviate from the eigen-value is given by

$$E' = \mathcal{J} \pm \mathcal{K}$$

where

$$\begin{aligned}\mathcal{J} &= \int (\psi_a(1)\psi_b(2)) * \frac{e^2}{4\pi\epsilon_0 r_{12}} (\psi_a(1)\psi_b(2)) d\vec{r}_1 d\vec{r}_2 \\ \mathcal{K} &= \int (\psi_a(1)\psi_b(2)) * \frac{e^2}{4\pi\epsilon_0 r_{12}} (\psi_b(1)\psi_a(2)) d\vec{r}_1 d\vec{r}_2\end{aligned}$$

[2] The spin term of the total wave-function has been omitted from the total wave function as the perturbation treatment is not dependent on the spin. More about the perturbation treatment can be found in *Spectrophysics, principles and applications* pages 30-31.

2.1.4 Many-electron systems

In analogy to the previous text, many-electron systems are when there are three or more valence electrons in the atom. This complicates things as the interaction term between the electrons becomes larger and more complicated. Hence this term will be a sum over all N valence electrons, just as there will be sums over the N electrons' kinetic and potential energies.

The Hamiltonian becomes

$$H = \underbrace{\sum_{i=1}^N \left(-\frac{\hbar^2}{2m} \nabla_i^2 - \frac{Ze^2}{4\pi\epsilon_0 r_i} \right)}_{\text{kinetic and potential energies}} + \underbrace{\sum_{i < j=1}^N \frac{e^2}{4\pi\epsilon_0 r_{ij}}}_{\text{exchange interaction}} + \underbrace{\sum_{i=1}^N \xi(r_i) (\vec{l}_i \cdot \vec{s}_i)}_{\text{spin-orbit interaction}}$$

Just as in the two-electron case, the SE is very hard to solve for this case. Other interactions that will affect the energies can be added to the Hamiltonian. However these are added as perturbations after finding the first approximation solution. [2] Solving the SE at this stage can be done using approximations and omitting terms to find a simpler solution and use perturbation theory to find the deviation from this. The first approximation that can be done is to omit the spin-orbit term but to keep the exchange term as at this stage it would not be a good approximation to treat this part of the Hamiltonian as a perturbation. The more electrons that are summed over, the larger the exchange term will be and the larger it gets, the worse a perturbation treatment would become. The second thing that can be done in order to simplify the evaluation of the Hamiltonian, is to make a few assumptions in order to simplify the exchange term. The first assumption is that the distance $r_{ij} = |\vec{r}_i - \vec{r}_j|$ can be approximated to be radial in order to receive a spherical symmetry. When doing this it can be further assumed that the distances in the atom are so large so that the electrons move independently of each other, so the potential that each electron feels only depends on the distance of the electron from the nucleus. The electrons behave as if they were in a central field and the exchange term can be made part of the potential energy and this simplified Hamiltonian becomes:

$$H = \sum_{i=1}^N \left(-\frac{\hbar^2}{2m} \nabla_i^2 + V(r_i) \right)$$

As in the two-electron case, which could be separated into 2 equations, the Schrödinger can be separated into N one-electron equations. [2] These will however be dependent on each other as the potential felt by one electron is dependent on the field created by the other electrons and the nucleus. In order to solve for one configuration the states of all the other electrons need to be known. The solution can be found by means of iteration, where one test-function is used to approximate all the electrons and from this the charge distribution and the central field potential can be found. This is then repeated until the result is within a tolerance to the previous. This is called the Hartree-Fock method. [2]

The solutions to these N Schrödinger equations will all have the same angular part as the one-electron system as these conditions are still the same. However, as the potential field is no longer the Coulombic field which was the case for one-electron systems, the radial part has changed. The total wave-function for the system will be the product of the one-electron functions and the total energy will be the sum of all the eigen-energies. Due to this non-Coulombic field the eigenvalues will not only depend on n as for one-electron systems, but it will also depend on the angular momenta l . This is due to that the field

the inner electrons create screen the nuclear charge from the outer electrons. This is seen in that the electrons with lower angular momenta and same n penetrate further into the charge distribution and as an effect of this feel a higher effective nuclear charge, and are more tightly bound to the nucleus. The electron configuration $n_N l_N$ helps to describe the energy eigenvalues for the central field approximation. As the total wave-function is the product of N wave-functions the parity is the sum of the angular momenta $\sum_i^N l_i$. [2] Recalling all the properties of some of the known quantum numbers, that

$$\begin{aligned} -s &\leq m_s \leq s \\ -l &\leq m_l \leq l \end{aligned}$$

then if the electrons fill up in the orbitals and sub-shells so these become filled, the components of the angular momenta will cancel out. For these cases the charge distribution will be spherically symmetric as all components cancel out. The parity will be the sum of the unfilled orbitals angular momenta as all the filled ones sums up to zero (due to the quantum number m_l). [2] *Spectrophysics, principles and applications* is recommended for further understanding of the perturbation treatment of the non-central part of the electrostatic interaction.

The observed energy levels are more complicated and cannot just be explained with the electronic configuration, and differ from the expected values. This is because the electrostatic interaction still has a non-central part and the spin-orbit interaction contributes to the energy. These were omitted in the central field approximation and can be added to the discussion through a perturbation treatment. The Hamiltonian that takes the electrostatic interaction into account is

$$H_{es} = H + \sum_{i < j=1}^N \frac{e^2}{4\pi\epsilon_0 r_{ij}}$$

i.e., the old Hamiltonian and the perturbation term. The total wave-function formed must follow the same set of rules as in the two-electron case, that the probabilities do not change during exchange of electrons, hence they stay symmetric or anti-symmetric. This can be achieved as mentioned before by constructing linear combinations of the product wave-functions. [2] The investigation of the perturbation gives that the contribution to the energy from the non-central part of the electrostatic interaction will be given as

$$E_{es}(LS) = \underbrace{\sum f_k F^k}_{direct} + \underbrace{\sum g_k G^k}_{exchange}$$

Where F^k and G^k are called Slater integrals. (More information about this can be found in *Spectrophysics principles and applications* pages 37-38.) So the energy without the perturbation will be altered twice by the above energy contributions. [2] How these affect the energy levels can be seen in Fig.3.

After this, the spin-orbit interaction need to be investigated, as this affects the energy levels in the sense that it splits them, the spin-orbit give the fine structure. This is the last part of the Hamiltonian

$$H_{so} = \sum_{i=1}^N \xi(r_i) (\vec{l}_i \cdot \vec{s}_i)$$

the spin-orbit perturbation term. The function $\xi(r_i)$ depends on the potential V , and is thus never the same for different systems. This interaction is related to the total angular momentum \vec{J} of the electrons, which is the sum of the total spin and angular momenta. This quantum number will take values in the interval $|L - S| \leq J \leq L + S$ and the values

of the total angular momentum will be, as the total angular momentum operator suggests, $|\vec{J}| = \hbar\sqrt{J(J+1)}$. Hence an energy level without spin-orbit will split into J-levels when spin-orbit is taken into account. To the total angular momentum a quantum number M_J is used, and for each J the energy level will have a degeneracy, or a *statistical weight* $g = 2J + 1$. [2] How the energy is shifted is given by the Landé interval rule, which states that the energy splitting will be proportional to the larger of the J values

$$\Delta E(J, J - 1) = A(LS) \cdot J$$

$A(LS)$ is the splitting factor for the system. [2] More about this splitting factor and spin-orbit interaction is dealt with in *Spectrophysics, principles and applications* pages 40-43. This treatment of the spin-orbit interaction is called LS coupling, and is valid only when this interaction is smaller than the non-central part of the electrostatic interaction. [2]

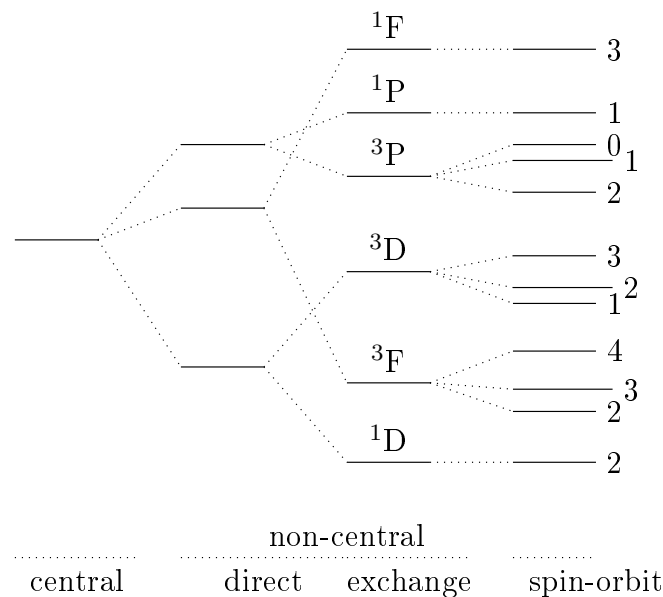


Figure 3: How the perturbation affects the energy levels.

The transitions that can occur have to obey a couple of transition rules, which can be derived from quantum mechanics. The spin cannot suddenly change, so $\Delta S = 0$. For a transition to occur $\Delta L = 0, \pm 1$. Hence a transition can only occur if there is a parity change. To these the rules $\Delta J = 0, \pm 1$ and $J = 0 \rightarrow J = 0$ can be added, where the latter one is strictly forbidden. [2]

2.1.5 Nuclear perturbation

The nucleus affects the energy structure of the atom. This is due to that the protons as the neutrons have spin as well. This yields a resultant spin of the nucleus \vec{I} and as in the electronic case this resultant spin will have an associated magnetic moment $\vec{\mu}_I$. [2] The magnetic moment will be

$$\vec{\mu}_I = g_I \frac{e}{2m_p} \vec{I}$$

The fact that the electrons have a charge and move about the nucleus creates a magnetic field, which the nuclear moment will interact with. This contributes to the atomic energy

levels, and will shift them, however this affect will be less than the fine structure. The perturbation, to this point evaluated Hamiltonian, will be

$$H_{HFS} = -\mu_I \cdot \vec{B}_J = C\vec{I} \cdot \vec{J}$$

which gives the perturbation energy

$$\Delta E_{HFS} = \underbrace{A}_{\text{constant}} \frac{1}{2} [F(F+1) - I(I+1) - J(J+1)]$$

where F is the new quantum number, which is defined to be $\vec{F} = \vec{I} + \vec{J}$, the total angular momentum of the atom. A is the hyperfine structure constant. This new quantum number F follows the same set of rules as the previous, hence $|I - J| \leq F \leq I + J$ where we have another quantum number M_F which is the projection of F , $-F \leq M_F \leq F$. [2] This quantum number gives the additional selection rules for a transition to occur

$$\Delta F = 0, \pm 1$$

$$F = 0 \rightarrow F = 0 \quad \text{not allowed}$$

[2]

In addition to the coupling between the nuclear spin with the magnetic field the electrons create, the shape of the nucleus affects the perturbation. The nuclear electric quadrupole-moment Q gives rise to a small deviation from the hyperfine structure. This is due to the shape of the nucleus, and $Q = 0$ when the nucleus has a spherical symmetry.

It can be mentioned that the reduced mass was only used in the evaluation of the one-electron case, it is used in order to correct the energy levels to the finite mass of the nucleus. For many-electron systems this reduced mass becomes more complicated. Using the reduced mass separates the kinetic energy, to one sum over the kinetic energy of the electrons and one sum of the nucleus moving relative to the systems common centre of mass. [2] Before only the first sum has been investigated. This has little effect on the energy levels, however is visible when comparing isotopes of an element. When performing the algebra of the now present kinetic energy and using the conservation of linear momentum give the *normal mass shift* of the two isotopes. This shift can of course be correlated to a shift in wave-number. More can be read about the nuclear affects of the nucleus in *Spectrophysics principles and applications* p 78-85. [2]

Isotopes of an element of course have different volumes and these also create an effect on the energy levels. This is because when the volume of the nucleus increases some of the orbitals, those with low l -level as those have higher probability to penetrate the nucleus, will penetrate into the nucleus and will feel a lower nuclear charge and be less tightly bound to the nucleus. [2]

2.2 Optical spectroscopy

Spectroscopy is the study of light by resolving the light into its components. This can be achieved for example using a prism, where it becomes evident that the refractive index of the material depends on the wavelength propagating through it. Other methods can involve the use of a grating. This is used in order to see the different components of the light. The investigation of the light emitted from a gas of atoms or molecules can tell us the energy levels of that specimen. Hence spectroscopy is useful in order to investigate matter.

2.2.1 Light sources

Different light sources have been developed for spectroscopy for various purposes. If an emission spectrum is to be investigated then the lamp contains the species under study. The name of these direct lamps are *line light sources*. [15] For a more general review of the different sorts of lamps that have been developed, see Sune Svanberg's *Atomic and Molecular Spectroscopy* pages 85-90.

For absorption spectroscopy it is more difficult to achieve absorption with a peaking wavelength lamp, such as the line light sources, since the intensity per spectral interval of the overlap has to be sufficient to excite the system. In order to achieve absorption *continuum light sources* can be used, as they will have a total overlap in wavelength. However, the intensity of the light might not be sufficient to excite the system. The probability of excitation increases if the absorption bands are broad, because then the integrated intensity over the spectral interval might suffice to excite the atom. *Lasers* have high intensity per wavelength interval and have a sufficiently high probability to excite the system.

The width of the received line gives the accuracy of the measurement. However, there are several contributions to the spectral line. The first contribution is the actual width of the light source and there will be a further contribution to this from the spectral instrument being used. [15] The other contributions will be from the motion of atoms and molecules in the specimen. [15] If ions and electrons are present the effect of the electrical field on the atoms will also contribute to the light. [15]

Natural broadening is the minimum spectral width and this is an effect of the Heisenberg uncertainty principle as the state of the system has a finite lifetime. [2]

Doppler Broadening arises due to the Doppler effect. It is an effect of the varying velocities and directions of movement of the atoms. Then the radiated light will be different for different atoms and the received light will be in an interval of wavelengths and different atoms will contribute to different parts of the spectral line. Some of the light will be red-shifted and some blue-shifted. The Doppler shift will be given by, if the emitter is moving in a velocity v_x towards the observer

$$-\frac{\Delta\lambda}{\lambda_0} = \frac{\Delta\nu}{\nu_0} = \frac{v_x}{c}$$

or

$$\Delta\nu = \nu_0 \frac{v_x}{c}$$

The number of atoms with velocity components between v_x and $v_x + dv_x$ is given by a Maxwell distribution

$$dN(v_x) = \frac{N}{\sqrt{\pi}\alpha} e^{-v_x^2/\alpha^2} dv_x$$

where α is given by

$$\alpha = \left(\frac{2kT}{m_A} \right)^{1/2}$$

k is Boltzmann's constant, T is temperature and m_A is the atomic mass. This is equivalent to $E_k = \frac{1}{2}mv^2$, so $v = \sqrt{\frac{E_k}{2m}}$. Hence α will be the "most probable speed" ². Then

²A. Thorne U. Litzén and S. Johansson, *Spectrophysics: Principles and Applications*, 2007, Media-Tryck Lund, p198

distribution can be written

$$dN(\nu) = \frac{Nc}{\sqrt{\pi}\nu_0\alpha} e^{-\left(\frac{c\Delta\nu}{\nu_0\alpha}\right)^2} d\nu$$

[2, 15] Using this and the FWHM (Full width half maximum of the spectral line) $\delta\nu_D = 2|\nu_{1/2} - \nu_0| = 2\sqrt{\ln 2} \frac{\nu_0\alpha}{c}$ will give a line profile $g(\nu)$

$$g(\nu) = 2\sqrt{\ln 2/\pi} \frac{1}{\delta\nu_D} e^{-4\ln 2 \left(\frac{\nu_0 - \nu}{\delta\nu_D}\right)^2}$$

The Doppler line profile will be

$$I = I_0 e^{-x^2}$$

,where I is the intensity of the line, and where

$$x = 2\sqrt{\ln 2} \frac{\nu_0 - \nu}{\nu_D}$$

[2, 15]

This effect can be limited by cooling of the specimen, so that the velocity range in which the atoms and molecules move, decreases. A slit could also be used in order to limit the Doppler width, as then light components of a small velocity in the line of sight can be selected. [2]

Pressure Broadening When the pressure increases in the specimen, collisions between the different atoms and molecules will become more frequent. [15] This will affect the broadening of the line, however the line profiles will be different from the Doppler distribution. [2]. Lorentzian broadening is a type of pressure broadening, and it is due to broadening of the spectral line due to collisions between different kinds of atoms. In the same way Holtzmark broadening is due to collisions between the atoms of the same element. [15] How the lines look depends on many factors, for example if the atoms are charged or if there are resonance interactions between identical particles present. [2] The pressure width can be calculated using

$$\Delta\nu_{coll}(P, T) = \Delta\nu_{coll} \frac{P}{P_0} \sqrt{\frac{T_0}{T}}$$

With increasing pressure, for example at atmospheric pressure, this effect becomes more dominant.

2.2.2 Optical resolution

Resolving the different components of the light is achieved by using instruments such as prisms and gratings. The resolving power and light transmission by the instrument are important factors for efficient resolution. The concept of resolving power of the instrument is constructed and is defined as

$$\mathcal{R} = \frac{\lambda}{\delta\lambda}$$

where $\delta\lambda$ is the line-width of the instrument and λ is the wavelength used. [15]

2.2.3 Grating spectrometers

Spectral separation is achieved by a grating, in a similar way as a prism does, however a reflection grating achieves this by its surface. The theory behind how the grating spectrometer works is based on light interference. Constructive interference occurs when the optical path difference between the interfering light is an integer value of the wavelength. If the optical path difference would take half integer values of the wavelength, then destructive interference occurs. The grating equation

$$m\lambda = d(\sin\alpha + \sin\beta)$$

where d is the distance between the grooves in the grating and the angles are the angles of incidence and reflection respectively. n is just an integer. The resolving power will be

$$\mathcal{R} = \frac{\lambda}{\delta\lambda} = N \cdot m$$

where N is the number of illuminated lines, and m is the diffraction order. [15] There are several types of gratings, and for the interested reader these are described in more detail in Sune Svanberg's *Atomic and Molecular spectroscopy* page 105. The intensity of the light reflected from the grating depends on the grooves of the grating. The shape determines how the light is reflected. [15] The use of mirrors and the shape of the grating surface depends on the spectral regions being investigated. For the X-ray region concave gratings are often of use. There will be stray light in the selected wavelength region. However, this can be reduced by the use of a double monochromator. [15]

2.2.4 The Beer-Lambert law

The Beer-Lambert law describes how incoming light on a sample of thickness b is attenuated when passing through the sample, where incoming light is of intensity I_0 and outgoing I_t . The length of the sample can be divided into pieces of length Δx , and what happens in the sample over this interval can be studied. The incoming light has intensity I_0 and the light will be reduced to I in the sample, then it will be reduced by ΔI over the interval Δx . This will give a fractional attenuation

$$\frac{\Delta I}{I} = -k_1 c \Delta x$$

where k_1 is a constant and the c is the uniform concentration of the sample. If the outgoing light has an intensity of I_t then the expression can be integrated since the boundaries are known [15]

$$\int_{I_0}^{I_t} \frac{dI}{I} = - \int_0^b k_1 c dx$$

with the solution

$$\ln \frac{I_0}{I_t} = k_1bc$$

. The ratio I_t/I_0 is defined as the transmittance T ³ so the expression can be restated as

$$\ln \frac{1}{T} = k_1bc$$

From this the *absorbance* can be defined

$$A = \log_{10} \frac{I_0}{I_t} = 0.434 \ln \frac{I_0}{I_t} = 0.434 \ln T^{-1} = k_2c$$

The *Beer-Lambert* law is thus equivalent to

$$A = 0.434k_1bc = k_2c$$

and states that the absorbance is proportional to the concentration of the sample. [15]

2.2.5 Detectors

Before the entry in the digital time the photographic plate was used in order to detect light. However, there have been many types of detectors developed to investigate spectral lines, for instance the CCD and the PMT. In this experiment both the PMT and the CCD are used, however the PMT is more effective in detecting light, so this section will deal with how the PMT works. The PMT (*Photo-Multiplier Tube*) is a photocell that amplifies the incoming light. This is achieved due to the photoelectric effect, as the incoming light excites electrons in the photo-cathode which are released from the atoms. The electrons are then accelerated due to an increasing potential field, and hits a series of dynodes, where at each electrons are knocked off. The signal becomes amplified due to this avalanche effect, and the obtained current becomes 10^6 times larger than the current from the photo-cathode. [15]

³Sune Svanberg, *Atomic and Molecular Spectroscopy: Basic Aspects and Practical Application*, 2nd edition, 1992, Springer-Verlag Berlin Heidelberg, p.133

2.3 Atomic Spectra

2.3.1 One-electron systems

The hydrogen atom is the simplest of all atoms, and is the simplest one-electron system. Observations of the atomic spectra of the hydrogen atom seem to be consistent with theory; that the radiation emitted from or absorbed by the hydrogen atom is compatible with the energy eigen-values known from the solution to the SE. The series of lines are well known and are called accordingly to their describer. The *Lyman* series is a series of lines where the electron de-excites to the lowest level in the atom with principal quantum number $n = 1$. This radiation is in the ultraviolet region. The *Balmer* series is radiation in the visible region and has $n = 2$ as its lower level. The higher levels with increasing quantum number n as lower level are in the infra-red region and cannot be observed easily. [2]

Other hydrogen-like systems, for instance ions such as He^{1+} and Li^{2+} belonging to the iso-electronic sequence, have similar atomic spectra to that of the hydrogen atom, however with the small adjustment of the energy levels, as the Coulomb field has changed due to that the number of protons have increased. The energy changes with Z^2 hence the energy transitions will be scaled with this factor. [2]

The alkali metals are one-electron systems since they fill the known criteria for the system. The filled shells are stable so the observed spectra from these have to be due to the valence electron. [2] Take Li as an example to help explain how the transitions work, as it is the first alkali metal. The ground state has electronic configuration $1s^2 2s$ so the next state, the first excited state should be in the same shell, however as parity has to change for a transition, and knowing that the angular momentum can only change by one, the next state is $1s^2 2p$. Now one of the perturbations affect the energy level, and this excited state thus splits into two. How we know this besides from observation, is that the multiplicity $2S + 1$ of the state is 2 and is this for all alkali metals, so is thus a doublet state. So the energy levels can be denoted $1s^2 2p \ ^2P_{1/2,3/2}$ where the latter part is the term that denotes the energy levels after taking spin-orbit interaction into account. The interested reader can find more information about spectral series in *Spectrophysics principles and applications*. The electron can be further excited to the next 3s state, and the configuration and term will change accordingly to $1s^2 3s \ ^2S_{1/2}$. From now on the latest part of the configuration only need to be written. These transitions occur when the atom are affected by an electromagnetic field and excites. When the atom de-excited it follows the same set of rules as for excitation, known as the electric dipole rules.

A short comment should be made about other types of one-electron systems in order to facilitate the discussion about the spectra from other two and many-electron systems. For some atoms the s^2 sub-shell, which is filled, is not as stable as for the case of the alkalis. "The energy needed for exciting one of the s electrons is relatively small" ⁴ [2] The configuration interaction is a perturbation to the non-central part of the electrostatic interaction which acts between different states that have the same quantum number L and S as J , but from different configurations of the same parity. This perturbation causes level shifts. In the transition metals the $(n+1)s$ electrons have similar energies to the nd and the configurations they form have the same parity. Consequently their energy levels mix and shifts due to their interaction. This can be seen in Al I with electron configuration $3s^2 3p$ and first excited configuration $3s 3p^2$. Four terms can be created to these configurations: $^2S, ^2P, ^4P$ and 2D . The configuration interaction affects these terms as they interact with other $3s^2 nl$ series with the same parity and L and S . [2]

⁴A. Thorne U. Litzén and S. Johansson, *Spectrophysics principles and applications*, 2007, Media-Tryck Lund, p 60

2.3.2 Two-electron systems

The Helium atom is the most basic two-electron system there is and has ground configuration of $1s^2S_0$. The first excited state is $1s2s^1S_0$, so excitations give configurations $1snl$ and the terms 1L and 3L . The parent configuration of this will be $1s$ and have the parent term 2S_0 . These transitions series converges towards the parent term $1s^2S_0$ which is the ground term for ionized Helium. Similar structures can be seen in the alkaline earth's and iso-electronic ions which have s-electrons as valence electrons. [2] A difference in this structure arises when the d orbitals start to be filled in the energy levels of the atom. Helium and the two first elements in the alkaline earth's share the same sort of behaviour as they have 2 s-electrons outside a stable $2p^6$ shell. From Sr and down in the period the d shell is filled and their behaviour becomes more transition-metal-like. They will behave more like displaced systems. For Ca the case is different if both of the $4s^2$ electrons are excited to the 3d as well as 4s since these are close in energy. Then there will be a new system $3dnl$ which is slightly higher than $4snl$. If the the nd and $(n+1)s$ have similar energies the system will probably become displaced, as the energy levels will affect each other. This makes the received spectra from two-electron systems more complex.

Systems where the valence electrons consist of two p-electrons, with a ground configuration ns^2np^2 , forming the terms $^3P, ^1D$ and 1S behave accordingly. When exciting the system the system takes configuration $npn'l$, forming possible singlet and triplet states with the parent term np^2P . If one of the s-electrons is excited so the electron configuration becomes $nsnp^3$, the possible terms for this scenario becomes $^2S, ^5S, ^2P$ and 5P . This will be visible in the spectra.

The noble gases can be treated as two-electron systems, even though they have no valence electrons. They have a ground configuration np^6 and exciting the system will give $np^5n'l$, where the parent configuration will be np^5 and have the parent term 2P . [2]

2.3.3 Complex systems

It is not only for many-electron systems which the spectra become all too complex; it is also for two-electron systems. So the discussion about the complex atoms (even though only two-electron systems) can be extended to many-electron systems. The first stage of complexity has been dealt with in two-electron systems as well as one-electron systems, when the energy levels affect each other and also the effect it has when the terms converge to the parent term. Next stage is whether there are more than one parent term to the configuration, and if these overlap with other parent systems. There may be identical LS terms with different energies, so the parent term is included in the term notation so different levels can be distinguished. [2] Soon the system becomes complex because each configuration has several parent terms that each split into several levels due to the spin-orbit interaction. The number of possible transitions that can occur in the system increases rapidly, so the observed spectra from p^k systems will be far from simple to investigate. [2]

The transition metals are atoms which have nd and $(n+1)s$ electrons whose binding energies are almost the same. Transition elements with d^k configurations will, depending on the circumstances, have a larger number of parent terms compared to elements with parent terms created by p electrons. The spectra is further complicated by the overlap of systems, which can occur if the configurations have similar energies. Depending on the parity, the situation becomes more complex if configuration interaction occur. The resulting terms of the systems are derived through the same method as before; by adding the angular momenta and spin of the nl electron to the parent term. [2] Due to this many of the lines in the spectra will lie in the same wavelength region.

If you have a systems with k equivalent electrons, the Pauli principle has to be taken into account when deriving the terms of the configurations of the other $k - 1$ electrons. Hence this is not done by adding l and s to the parent term. In order to treat these types of cases theoretically, fractional parentage describes the relations between the terms of configurations l^k and l^{k-1} . [2]

2.4 Conclusion

What has been explained previously to this can be used when investigating different elements and molecules, because they have their own distinct energy levels. In other words, when light interacts with the specimen investigated, and the light corresponds to the energy difference between ground state and the first excited state the specimen might be excited. Excitation occurs if the perturbation the field exerts on the atom fulfils the condition of the wave-function. The outgoing light intensity will decrease because quanta is absorbed.

The element used in this experiment is mercury, with electron configuration $[\text{Xe}] 4f^{14}5d^{10}6s^2$ where the $6s^2$ are valence electrons. Thus the mercury atom can be treated as a two-electron system. The first excited state of mercury is $[\text{Xe}] 4f^{14}5d^{10}6s6p$ and thus will have the parent configuration $6s$ and the parent term 2S . The first excited terms will be 1P_1 and $^3P_{0,2}$. Exciting the system further will give more terms. However it should be noted that the nd and $(n + 1)s$ electrons have similar binding energies and therefore depending on the circumstances, like how the systems is affected in order to be excited, the first excitation might be $[\text{Xe}] 4f^{14}5d^96s^27s$. The case might be so that the $6s$ electron is first excited and then the $5d$ electron and the system will have configuration $[\text{Xe}] 4f^{14}5d^96s^26p$. This would give complicated terms and these would have similar energies. So depending on how the system is excited and which electrons are excited the spectra will reveal this, as the emitted light will correspond to the energy level and hence which configuration the system has been excited to.

In this investigation the transition $6s6p^3P_1 \leftrightarrow 6s^23S_0$ corresponding to 2537 \AA , will be investigated using absorption spectroscopy. Mercury will have isotope shifts due to mass effects and nuclear spin, however due to the experiment not being that sensitive this cannot be rendered here.

2.5 LED (*Light emitting diode*)

In order to fully explain how the *light emitting diode* (LED) works, some basic concepts in *Solid State Physics* have to be explained. The first concept is the conduction properties of materials. Conducting materials have free electrons that are free to move about randomly. When the material is subjected to an electric field, the electrons start to move in one direction. These materials are often ionic solids, because they have tightly bound electrons in the ionic bond and some free electrons. The metallic bonding is even more efficient when it comes to conduction because the valence electrons are the free electrons in this case. There are some cases where the valence electrons are more tightly bound, and the electrons can only move to a certain extent, and contribute to a current flow. These are the semiconductors. [6] How well the material conducts electricity is called the *electrical conductivity* ρ and the reciprocal of this property is called the *resistivity*. This property relates to the resistance of the material, and the resistance gives how easily the electrons flow through the material. [6] The resistivity originates from vacancies, dislocations and impurities in the material, such as grain boundaries. [6] The electron mean free path is the the distance an electron can travel in the material before encountering an obstacle, under the influence of an electric field. [6] This is also governed by the Pauli exclusion principle, because the electron can only have a certain value on its wavevector after a collision, which limits the number of possible collisions. [6]

To understand why some materials are conductors and others are not, the concept of energy band formation has to be dealt with. Imagine what happens when a large number of atoms come closer together from a very large distance. Their electronic wave-functions start to overlap and this interaction splits the degeneracy of the energy levels and causes them to form a band of energy levels which the electrons can place themselves in. This describes what happens in a metal or ionic solid where the atomic spacing is very small compared to that of a gas. In a gas the atoms are isolated and have their electrons in the same levels without violating the Pauli principle. The energy band formation of solids prevent the Pauli exclusion principle from being violated which it otherwise would be as the atoms are not isolated from each other. The bands formed provide separate states for the electrons with the same set of quantum numbers. [6] The energy gaps in between the bands are present due to that there are regions with no energy levels in the isolated atoms. In the energy gaps no electrons can be. The band structure determines whether the solid is a conductor, or an isolator. This model that describes the energy bands is called the *tight-binding model* and more can be read about energy bands in Ann Holgate's book *Understanding Solid State Physics* p 158 and onward. [6] For conductors it is only the electrons in the outermost energy band that can take part in conduction and this happens easier if the energy band is far from full. This is known as the conduction band. The valence band is the band where the valence electrons are and this band is full. Semiconductors and insulators have a valence band and an empty conduction band. The difference between insulators and semiconductors is the size of the band gap between these two levels. [6] There are some concepts that need to be explained to fully discuss semiconductors, and these are the Fermi energy and level. Simply put, the Fermi energy is the energy of the highest filled state in an element. The Fermi level is the energy level where the probability distribution of the energies $F(E)$ will be $1/2$ ⁵.

Semiconductors are easily affected so they can conduct because the size of the band gap is small enough for electrons to be thermally excited to a higher energy state over the band gap. Adding impurities into the material also affects the conducting properties of

⁵Sharon Ann Holgates, *Understanding Solid State physics*, p197

the semiconductor. Semiconductors are divided into two groups, intrinsic semiconductors which is when the semiconductor is pure without impurities and extrinsic semiconductors which have impurities added. [6] The naming of the semiconductors is according to which group in the periodic table the component elements belong to. The LED used for this investigation is an AlGaIn semiconductor, and is therefore III – V as Al and Ga are both in group three and N is in group five. The thermally excited electron leaves a hole in the valence band. [6] The semiconductors are doped in order to increase the conductivity. This can be done by adding a material with more valence electrons than will be taking part in the binding. This is called *n-type* doping as the charge carriers will be electrons. If the dopant has fewer valence electrons then holes will be created and the semiconductor will be *p-type* as the holes are the charge carriers. The semiconductors as a whole are electrically neutral. [6]

The formation of the p-n junction is important for the LED. The p-n junction is created when n-type and p-type semiconductors are put together and diffusion of the different charge carriers take place. The n-type semiconductor will then be positively charged at the junction as the electrons will leave behind ionised atoms. The p-type semiconductor will be negatively charged as the holes will leave negatively charged ions behind. The region over which this potential difference occurs is called the depletion region. [6] When the potential difference has been established, electrons need to climb this potential barrier and the net flow is inhibited. An electric field is established due to the flow of the electrons and holes. This creates in turn a drift current which is in the opposite direction of the diffusion of respective charge carrier. At thermal equilibrium and no applied voltage over the junction, the net current will be zero. [6]

Applying a reversed bias potential across the p-n junction (the positive pole to the n-side and the negative pole to the p-side) will cause electrons to flow from the n-side to the p-side, and vice versa for the holes. There will be as a result to this bias more ionised donor and acceptor states and the junction voltage increases due to these additional states. The depletion region increases. Due to the increase in potential the probability for current flowing through the junction decreases. Hence the reverse-biased p-n junction has a very high resistance. [6] The opposite of this is the forward bias (where positive pole to the p-side and negative pole to the n-side) charge carriers will be added to both sides of the junction, holes to p-side and electrons to the n-side. The ions will recombine with these and the donor and acceptor states decrease. The depletion region will decrease in size and the junction potential difference will decrease. The probability for a current flowing across the potential increases due to this. As the electrons diffuse over the junction, a current is produced and hence the resistance for the forward bias case is less than in the unbiased case as opposite reverse bias case. [6] Connecting the p-n junction to a circuit creates a diode, which is famous for the two types of resistance it possess, depending on the direction in which the potential difference is applied. [6]

Now we are ready to have the discussion about LED. The diode is a p-n junction made from a direct gap semiconductor. Under forward bias electrons and holes recombine when they have diffused over the junction. When the electrons and holes recombine photons will be emitted. This occurs due to electrons present in the conduction band undergoing recombination with the holes in the valence band. In order to achieve this, the electron has to loose energy by emitting a photon to be able to end up in the energy state corresponding to the hole. Increasing the bias current more carriers will be produced and more recombinations will occur and hence the intensity of the light emitted increases with the potential. The colour of the emitted light depends on the band gap, as the wavelength is dependent on this energy difference. The band gap is different for different materials. [6]

3 Method

With the use of a LED, which consists out of an array of LED chips, a cell containing Hg will be illuminated in the wavelength region between 250 and 265 nm. This is done in order to try to detect the absorption line of mercury at 2537 Å with this type of light source, as a feasibility study; if the absorption band is found a series of concentration measurements will take place. From the beginning the plan was to use the set-up presented in Fig.5; however performing the measurements using this set-up proved non-trivial. Part of the task also consists of optimizing the set-up so the experiment can be performed. The process towards constructing the set-up and the physical effects seen at each step will be discussed. Performing the steps towards a method proved to be lengthy and difficult due to the unexpected behaviour of some of the equipment. An experiment with another type of light source was performed in order to illustrate the difficulties and differences between the two sources. First, the instruments for the primary investigation will be described, then the two parts of the investigation -each with a different source of light- where the differences will be illuminated.

3.1 Instruments

- Square wave generator
- LED driver
- LED
- Pin hole or optical fibre for UV-region
- Grating 2400 1/mm or 18001/mm
- Cell containing mercury, and a heat fan to control the temperature
- Parabolic mirror, later changed to a focusing lens
- Slit
- PMT
- OceanOptics Spectrophotometer for the UV-region
- DAQ card

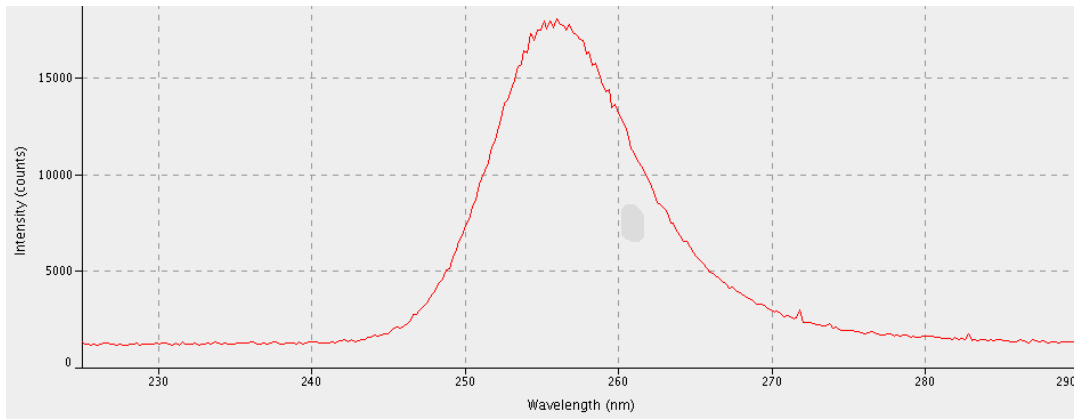


Figure 4: The spectral distribution of the LED

The radiated light originates from a nine point array, and the light source thus has a non-Gaussian line profile. The choice of light source instigate a couple of difficulties, which will be discussed later, the line profile being one of them.

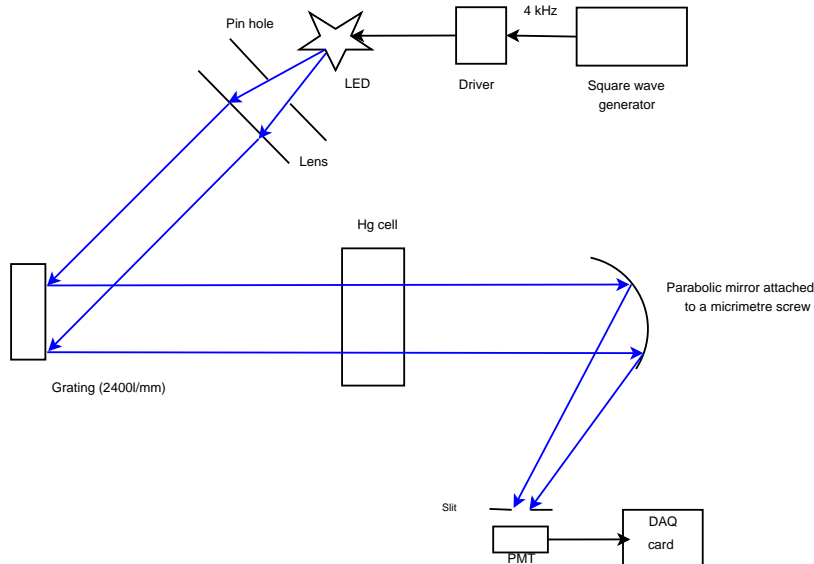


Figure 5: The original set-up

One of the orders of the dispersed light by the grating is chosen to pass through the mercury cell and is thereafter refocused by the parabolic mirror. Using the 2400 1/mm grating proved to only have zeroth, 1st and 2nd order dispersion, while the 1800 1/mm had up to 3rd order. Thus the 1800 1/mm grating is to be used because it can achieve higher resolution.

Using the mirror to focus the light instead of a lens should be more effective because the focal point of the mirror is independent of the wavelength; thus no chromatic aberration using the mirror. After the mirror the light passes through a slit before entering the PMT which is used to detect the light. Higher resolutions also means less transmitted light so consideration has to be taken when choosing order and the distance between the grating and the parabolic mirror. A longer distance between the grating and mirror will give a higher resolution, however the further they are apart the weaker the light becomes. Thus consideration about high resolution and a good signal-to-noise ratio has to be taken. The parabolic mirror is in turn attached to a micrometre screw so that the wavelengths can be scanned over, as the light from the LED is just not one wavelength.

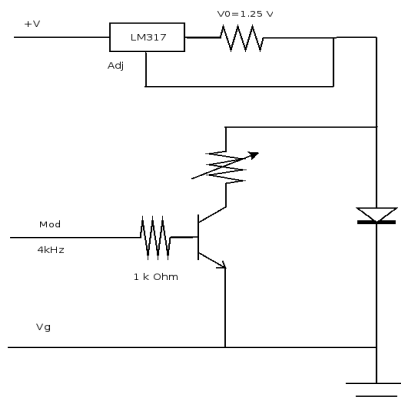


Figure 6: Driver circuit to the LED

The LED in this investigation is very sensitive. The current flowing through the LED is an exponential function of the voltage applied across the LED. Hence a small fluctuation of the voltage can give a huge fluctuation of the current. Fig.6. shows the driver circuit used in order to stabilize the current through the LED. The constructed chip evolved over three generations in order to get it to perform its task.

3.2 Fluorescence detection of Hg using level crossing spectroscopy set-up

This experiment is performed in the LTHs course "*Atomic and Molecular spectroscopy*". However, the method of the experiment is changed slightly as it is not the level crossing spectroscopy that is of interest in this investigation. The behaviour of the emitted light that occurs when the cold finger of the cell is cooled down with liquid nitrogen is what is observed in the investigation, and the curve that is generated when the finger is allowed to be reheated. The intent was to record the intensity and to note the discrepancy between the measured temperature and the actual temperature in the cell. Mercury is a heavy atom, there should hence be some time between changing the temperature of the cold finger of the cell and the mercury vapour reaching equilibrium.

What is relevant for this investigation is the knowledge that the light source is a mercury lamp that radiates light of wavelength 2537 \AA . The illuminated cell is placed before a filter and a PMT. The signal from the PMT is recorded and the behaviour is envisaged through a printer. This curve is then categorized and the concentration follows the Beer-Lambert law.

3.3 Investigation using a LED source for absorption measurements

The first step in this investigation is to find the absorption band of mercury. This is the difficult step to perform no matter which line of action is employed in order to find it.

3.3.1 Method 1

One of the methods is using the set-up described in Fig. 5 after first trying to isolate one of the array points with a pin-hole and collimate the light with a lens. This is one of the methods that can be used in order to achieve a Gaussian line profile. The signal from the PMT is viewed on an oscilloscope, while the spectrally decomposed light is scanned by the parabolic mirror. The signal-to-noise ratio should be high and using a filter should reduce the background. However this was not observed. Later this was assumed to depend on a faulty oscilloscope, with a constant high noise level. The absorption dip, which is the sought pattern of the signal, was hard to see and might be hiding in the noise. The noise can however be reduced by averaging the signal, which improves the signal to noise ratio. However, the absorption dip still was hiding in the noise. This was a time consuming method, because the averaging takes time. When scanning the intensity the dip should be recorded, because the intensity is Gaussian. The absorption band should then be found when the amplitude stays the same for a couple of scans, or if scanning along weaker intensities, decreases then increases before decreasing further. The noise makes this difficult to note. Noting the proper amplitude of the square wave on the oscilloscope is difficult. The width of the absorption band is very narrow so in order to obtain a broadening of the recorded absorption band, the cell could be heated in order to saturate the mercury and achieve pressure broadening of the line. Another method, as the heating would require an element that monitors the temperature, is to use a battery of cells the light can pass through. The higher the concentration, the wider the absorption line becomes due to broadening effects. However, the more cells that are used, the less intense the light will become and the voltage applied on the PMT needs to be increased.

A strange effect was seen when the scanning over the wavelengths was performed. The observed pattern seemed to resemble an interference pattern. This could be caused by a couple of things, amongst them if light from another array point on the LED passed through the pin hole and caused another order of light that interferes constructively with the order under investigation. The initial idea was if the mercury cells screened the light and caused the pattern due to obstruction. However, the pattern repeated itself when the cells no longer were present in the beam path. Hence, the cells were not the problem. It could be that the mirror truncates the beam.

The most plausible reason for the occurrence of this interference-like pattern is the parabolic mirror used. The mirror is diamond-machined, which causes grooves on the reflecting surface, which in turn can cause light interference in a similar manner to the ruling of a grating. This behaviour is unwanted but cannot be avoided.

At this point the method to produce a Gaussian profile evolved and a multi-mode optical fibre was introduced in order to collect the light from the LED and re-spread collimated light. Now the light from the array was collected and appears to be one integrated light source. An advantage with the fibre is that more light from the LED matrix can be used. The first step in evolving the experiment was now taken and the set-up changed to what is presented in Fig.7. This light should now have a Gaussian distribution which results in well defined orders. No orders could be created that could interfere with the order under investigation. Still the pattern occurred when the scanning was performed. Hence there is a high probability that the mirror is what gives rise to this pattern. Hence another

approach has to be used in order to find the absorption band.

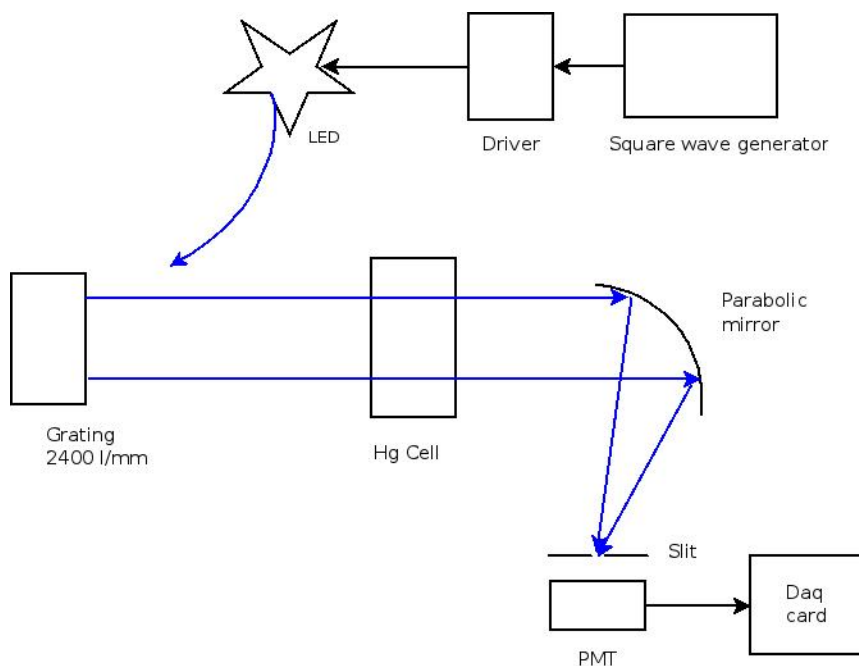


Figure 7: Version 2 of the experimental set-up

This method would be to use a spectrometer sensitive for the UV region in order to calibrate for the wavelength and detect the absorption band. The first step in evolving the experiment was now taken and the set-up changed to.

3.3.2 Method 2

Using what was learnt from performing method 1, the set-up evolved. In order to find the absorption band it was decided to use a spectrometer. Hence the spectrometer could be used to find the 254 nm wavelength, and the the slit and the PMT could be used in order to perform the concentration measurements, when using a well functioning oscilloscope.

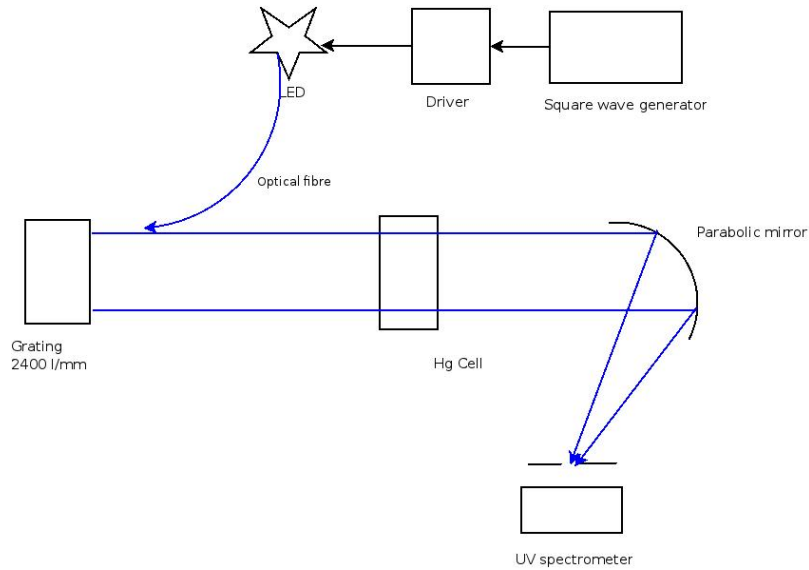


Figure 8: Version 3 of the set-up, to find the absorption band

The spectrometer uses a CCD to detect the light, which makes it possible to detect a whole wavelength range simultaneously. However, it should be noted that the CCD is not as sensitive to detect radiation as the PMT. The slit is deemed redundant at this stage, because the fibre that collects the light has an opening of $50 \mu\text{m}$, even though the slit can be made smaller than this, however this would affect the integration time on the CCD. This would increase the background, and it seems wise to minimize the background.

Using the spectrometer was not trivial and the method in order to find the absorption band of mercury had to be refined. The mirror was now used in order to collect the light into the spectrometer fibre. However the signal was still very weak.

It seems as the fibre opening is too small, that the mirrors beam width is not sufficient enough, which makes it difficult to place the spectrometer opening at the focal point. Another approach has to be used in order to focus the light, to get a stronger signal. Another method would also be beneficial because the truncation of the beam by the mirror cannot be eliminated. The truncation versus the negative effects due to dispersion by a lens had to be considered. At this stage a lens was introduced as it proved to allow to focus the light more effectively, even though the effects of dispersion cannot be eluded.

The signal became stronger after this, which had an impact on the integration time which could be reduced to 1 second from previous 10 s. Having the optical fibre collecting the light to the spectrometer attached to a positioner that could be translated along the line of sight of the beam enabled the wavelength to be scanned.

The optimal distance between the LED-fibre and the grating was found to be about 30 cm because higher resolution should result from more lines illuminated on the grating. The more the light is diverged before interfering with the grating the more lines will illuminated.

What was most efficient, could be found by investigation. The distance between the lens and the grating was increased to 1 meter and the effect of it was observed. The FWHM was reduced to about 2.2 nm. There are two possible ways to achieve higher resolution. The fibre thickness of the optical fibre which guides the light from the LED and spreads it to the grating is $400 \mu\text{m}$. The fibre collecting the light to the spectrometer has an opening of $50 \mu\text{m}$. This will give rise to a larger FWHM at 1m than if the guiding fibre was thinner. Thus higher resolution can be achieved by removing the collimating lens at the end of the fibre, and replace it with a slit, which could be made smaller than $400 \mu\text{m}$. Then the light

could be collimated with a lens. However this method would have the disadvantages that the signal would become very weak, as less light is used. Another disadvantage is that it might be difficult to illuminate the whole grating, and lower resolution would result from this. This was pursued but the signal became very poor so other methods tried instead.

The other method to achieve higher resolution is to minimize the effects of the optical fibre by decreasing the width of the fibre. Increasing the distance, which should give higher resolution, proved not to improve the resolution, which could be because the fibre reduces the resolution.

The set-up that seems to yield the best resolution is when using the formulated set-up to this point, even though it has some disadvantages. However this set-up can be improved by the choice of optical fibre guiding the light from the LED and directing it towards the grating.

Hence, presently the optimal method with the best performance is illustrated in Fig.9

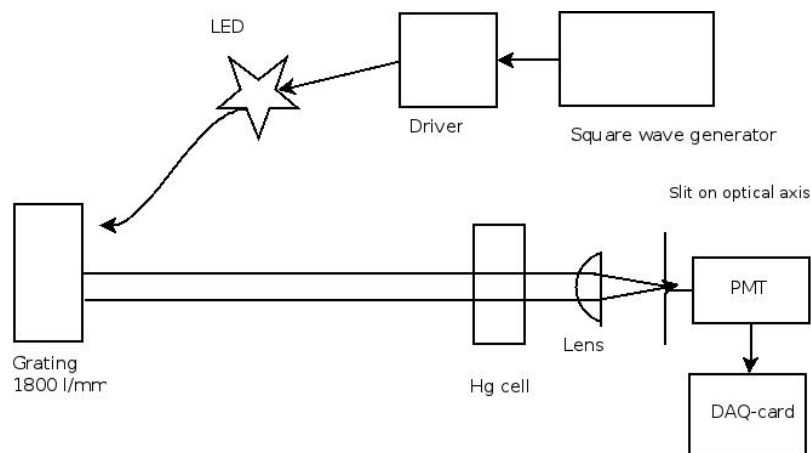


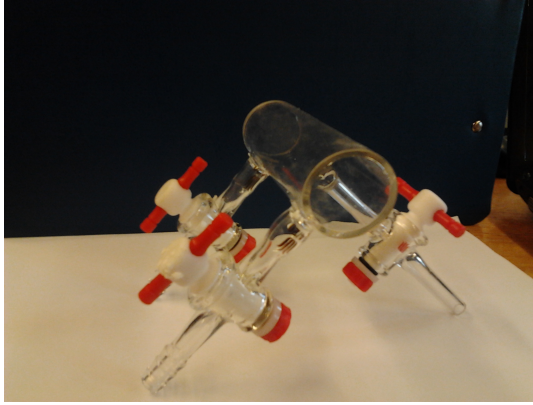
Figure 9: Final set-up

After adjusting the set-up and observing the absorption line of mercury the concentrations of the Hg-vapour in the gas cells at different temperatures can be measured, using the Beer-Lambert law.

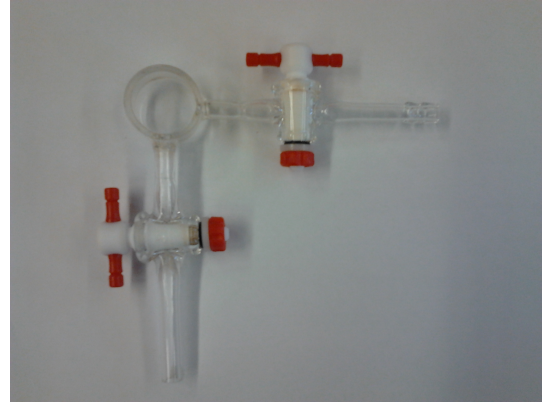
3.3.3 Experiment

The set-up constructed to this point can be used for the mercury concentration measurements. Now there are two incentives, the experiment we would like to do, and what we can do. We would like to perform concentration measurements using a PMT and a data acquisition (DAQ) card to record the signal. The designs of the cells to be used are depicted in Fig.10.

The mercury concentration will in these cases be monitored by pumping the gas into the cells, and the concentration does not have to be monitored by a cold finger. In the Anderson's design cell, Fig. 10 a, there is an outlet that is supposed to be connected to a vacuum pump and a pressure meter, the other is an inlet for buffer gas. The third arm is an extended sealed tube where the mercury will be present. Our design will have just an extended arm to put the mercury and an inlet that can either be connected to buffer gases, the vacuum pump or a pressure meter. The material the cells are made of are of course in quartz and fused silica in order for radiation in the UV to be able to propagate through it. The intensity difference would then be monitored, and through this



(a) Anderson's Design *Appl. Phys B* 87,341-353 (2007)



(b) Our Design

Figure 10: Cell designs for Hg vapour measurements

the concentration can be determined by using the Beer Lambert law, linking the absorption of the light to the concentration.

However, at this point we try to perform the measurements using the spectrometer instead, even though it is not as sensitive as the PMT. None of the above mentioned cells was used, as a cell with a small amount of mercury in a cold finger was used instead. The temperature of the cell will then be regulated by dipping the cold finger in liquid nitrogen. Intensity measurements will take place while the cell cools and heats.

During the execution of this it seems as the LED is not stable or needs time in order to stabilize. The intensity increases with time. This behaviour seems some what contradictory to how a LED work, because the warmer the LED gets the less the power output. 40 minutes was given to stabilize. The values seemed to stabilize and vary with 0.8%. After this the finger of the used cell was cooled with liquid nitrogen. The finger was not put directly into the nitrogen, in order to avoid thermal expansion of the material. The finger was allowed to cool down due to cooler environment.

3.4 Table of contents

$t/^{\circ}C$	Vapourpressure/Pa
-30	$637 \cdot 10^{-6}$
-20	$2.41 \cdot 10^{-3}$
-10	$8.08 \cdot 10^{-3}$
0	$24.7 \cdot 10^{-3}$
10	$65 \cdot 10^{-3}$
20	$160 \cdot 10^{-3}$
30	$370 \cdot 10^{-3}$
40	$810 \cdot 10^{-3}$
50	1.69

Table 1: The vapour pressure of mercury at different temperatures [8]

4 Results

4.1 Fluorescence detection

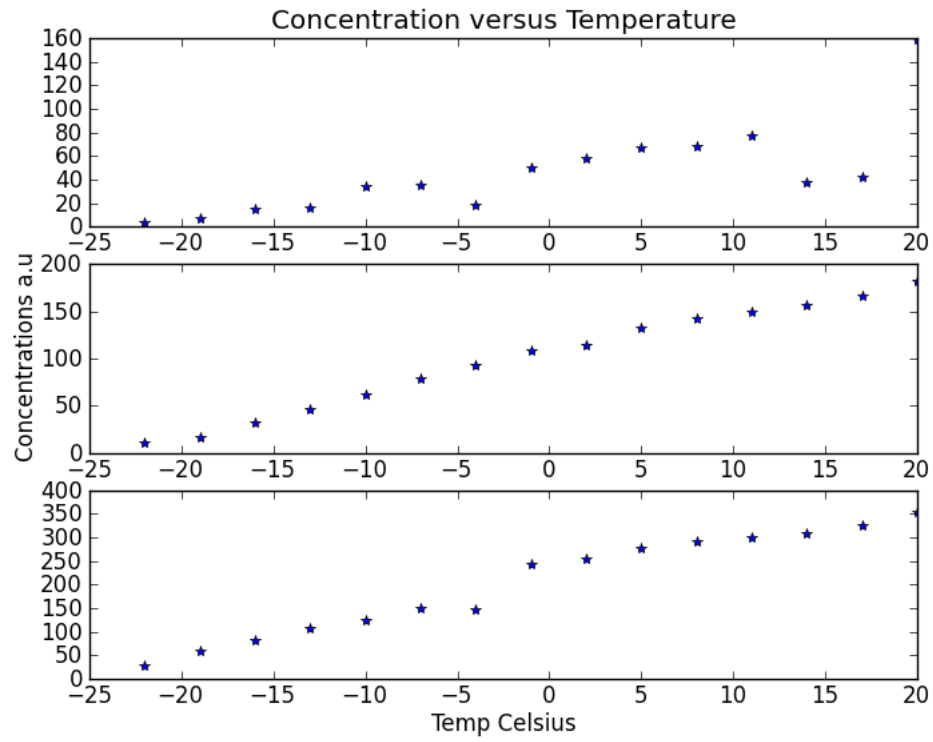


Figure 11: Concentration vs temperature

T°C	T°mV	Concentrations a.u		
		1	2	3
20	0.0	159*	182	355*
17	0.1	41*	166	327*
14	0.2	37*	156	309*
11	0.3	77	149	301*
8	0.4	68	143	293*
5	0.5	66	132	277*
2	0.6	58	114	254*
-1	0.7	49	108	244*
-4	0.8	18*	93	148*
-7	0.9	35	78	149
-10	1.0	33	61	123
-13	1.1	16	45	107
-16	1.2	14	31	82
-19	1.3	7	16	59
-22	1.4	4	10	27

Table 2: The concentration of measurements at different temperatures. The values marked with * are not average values. These concentrations should be multiplied by a constant.

4.2 LED absorption measurements

Saturated Number counts	Cooling Number counts
3176	3193
3180	3182
3165	3209
3180	3186
3177	3182
3171	3188
3188	3173
3186	
3203	
3183	
3188	
3183	

Table 3: The result of measurement

5 Evaluation and Discussion

Research on LEDs are being performed so in the future LEDs with enhanced performance will be developed. This investigation should be seen as a feasibility study and the experiment can be improved in future.

The absorption measurements achieved through the fluorescence detection experiment seem correct, even though the results have to be calibrated. The concentration decreases with the temperature decrease, which was expected. The experiment was not trivial to perform due to the deposition of the mercury in the cell which needs to be in the cold finger so the temperature in the cell can be controlled by the temperature of the finger. Also the Hg lamp had to be stable in order to perform the measurements, and this took some acquirement to receive. However the absorption measurements were easier to achieve because the light source has a width in the order to magnitude of \AA , which corresponds directly to the investigated wavelength.

The primary investigation was far from trivial to execute. The optimal settings were hard to achieve, and seemed impossible sometimes. Learning to use the instruments has been a journey too. As have been presented, many difficulties have been encountered during the performance. These directed the experiment in the different directions and lines of thought; some proved to be completely wrong whilst others correct. The performed experiment seems to have given no result, however this can be argued to depend on a number of factors. In the experiment presented the signal might not be seen because we have not achieved a high enough resolution, hence too large an area is integrated over. The possibility is thus that there is too much light to notice the difference in intensity; and even if there is a signal to be noticed it might be hidden in the noise and fluctuation of the background. Averaging the signal should reduce the signal to noise ratio (SNR) and take the background into account. However still no distinct signal can be interpreted from the data. If this is because the LED is not stable enough, the temperature of it should be monitored using a peltier element. This had been taken into account, however our specimen broke. So a future improvement is to use a working peltier.

This investigation could be argued to be a proof of principle, to try to achieve results now when the LEDs in the UV region are not as good as the cousin LEDs in the visible region and using the equipment provided of today. By this investigation knowledge is gained about the possibilities and challenges using UV LEDs for the detection of mercury. Future advances in LED technology means that the investigation can be improved in the future and the brute force behind the method has already been performed. Even though no signal was seen this method can be extended and be worked further with in the future in order to achieve results.

6 Appendix

6.1 Appendix A

$$H\Psi(\vec{r}) = E\Psi(\vec{r})$$

$$H = \underbrace{-\hbar^2 \frac{\nabla^2}{2\mu}}_{\frac{p^2}{2\mu}} - \underbrace{\frac{Ze}{4\pi\epsilon_0 r}}_{V(r)}$$

$$\nabla^2 = \frac{1}{r^2} \frac{\partial}{\partial r} \left(r^2 \frac{\partial}{\partial r} \right) + \frac{1}{r^2 + \sin^2 \theta} \frac{\partial}{\partial \theta} \left(\sin \theta \frac{\partial}{\partial \theta} \right) + \frac{1}{r^2 \sin^2 \theta} \frac{\partial^2}{\partial \phi^2}$$

$$\Psi(r, \theta, \phi) = R(r)Y(\theta, \phi)$$

$$\left[\frac{1}{r^2} \frac{\partial}{\partial r} \left(r^2 \frac{\partial}{\partial r} \right) + \frac{1}{r^2 \sin^2 \theta} \frac{\partial}{\partial \theta} \left(\sin \theta \frac{\partial}{\partial \theta} \right) + \frac{1}{r^2 \sin^2 \theta} \frac{\partial^2}{\partial \phi^2} \right] R(r)Y(\theta, \phi) = \frac{2\mu}{\hbar^2} (E - V(r)) R(r)Y(\theta, \phi)$$

$$\left[\frac{\partial}{\partial r} \left(r^2 \frac{\partial}{\partial r} \right) + \frac{1}{\sin^2 \theta} \frac{\partial}{\partial \theta} \left(\sin \theta \frac{\partial}{\partial \theta} \right) + \frac{1}{\sin^2 \theta} \frac{\partial^2}{\partial \phi^2} \right] R(r)Y(\theta, \phi) = \frac{2\mu r^2}{\hbar^2} (E - V(r)) R(r)Y(\theta, \phi)$$

separating into radial and angular part.

$$\left[\frac{\partial}{\partial r} \left(r^2 \frac{\partial}{\partial r} \right) + \alpha \right] R(r)Y(\theta, \phi) = \frac{2\mu r^2}{\hbar^2} (E - V(r)) R(r)Y(\theta, \phi)$$

which give the radial

$$\left[-\frac{r}{R(r)} \frac{d^2}{dr^2} (rR(r)) + \alpha \right] = \frac{2\mu r^2}{\hbar^2} (E - V(r))$$

and angular

$$\left[\frac{1}{\sin \theta} \frac{\partial}{\partial \theta} \left(\sin \theta \frac{\partial}{\partial \theta} \right) + \frac{1}{\sin^2 \theta} \frac{\partial^2}{\partial \phi^2} \right] Y(\theta, \phi) = -\alpha Y(\theta, \phi)$$

and separating further

$$Y(\theta, \phi) = \Theta(\theta)\Phi(\phi)$$

give

$$\frac{\frac{1}{\sin \theta} \frac{\partial}{\partial \theta} \left(\sin \theta \frac{\partial}{\partial \theta} \right) \Theta(\theta)\Phi(\phi)}{\Theta(\theta)\Phi(\phi)} + \frac{\frac{1}{\sin^2 \theta} \frac{\partial^2}{\partial \phi^2} \Theta(\theta)\Phi(\phi)}{\Theta(\theta)\Phi(\phi)} = -\frac{\alpha \Theta(\theta)\Phi(\phi)}{\Theta(\theta)\Phi(\phi)} \Rightarrow$$

which separates to

$$\left[-\frac{1}{\sin \theta} \frac{d}{d\theta} \left(\sin \theta \frac{d}{d\theta} \right) + \frac{m^2}{\sin^2 \theta} \right] \Theta(\theta) = \alpha \Theta(\theta)$$

and

$$\frac{d^2 \Phi(\phi)}{d\phi^2} = -m^2 \Phi(\phi)$$

where the latter one has the solution

$$\Phi(\phi) = e^{im\phi}$$

which is single valued as it repeat its value for every 2π , but only if m take integer values.

7 References

- [1] T.N Anderson, J.K Magnuson, and R.P Lucht. Diode-laser-based sensor for ultraviolet absorption measurements of atomic mercury. *Applied Physics B*, 2007.
- [2] A.Thorne, U.Litzén, and S.Johansson. *Spectrophysics principles and applications*. Mediatryck, 2007.
- [3] H. Edner, A. Sunesson, S. Svanberg, L. Unéus, and S. Wallin. Differential optical absorption spectroscopy system used for atmospheric mercury monitoring. *Applied Optics*, 25(3), 1986. 403-409.
- [4] Hans Edner, Gregory W. Faris, Anders Sunesson, and Sune Svanberg. Atmospheric atomic mercury monitoring using differential absorption lidar techniques. *Applied Optics*, 28(5), 1 March 1989.
- [5] T. Hadeishi, D. A. Church, R. D. McLaughlin, B. D. Zak, M. Nakamura, and B. Chang. Mercury monitor for ambient air. *Science*, 187(4147), 1975. 348-349.
- [6] Sharon Ann Holgate. *Understanding Solid State Physics*. Taylor & Francis Group, 2010.
- [7] J.Alnis, U.Gustafsson, G.Somesfalean, and S.Svanberg. Sum-frequency generation with a blue diode laser for mercury spectroscopy at 254 nm. *Applied Physics Letters*, 76(10), 6 March 2000.
- [8] Gilbert Jönsson. *Grundläggande fysik om gaser och vätskor*. Studentlitteratur. Sweden, 1998.
- [9] Kemikalieinspektionen. Kvicksilver. <http://www.kemi.se/Content/Infocus/Mercury/Start>, Hämtad 2012-06-15 kl 13.00, 2011-01-21.
- [10] Kenneth S Krane. *Introductory nuclear physics*. John Wiley & Sons.Inc, 1998.
- [11] Livsmedelsverket. <http://www.slv.se/sv/grupp1/Risker-med-mat/Metaller/>, Hämtad 2012-06-15 kl 14.02.
- [12] Xiutao Lou, G.Somesfalean, S.Svanberg, Zhiguo Zhang, and Shaohua Wu. Detection of elemental mercury by multimode diode laser correlation spectroscopy. *Optics Express*, 20(5), 13 Feb 2012.
- [13] Kemikalieinspektionen Nylander.A. Kvicksilver i lågenergilampor och lysrör, tidtabell för utfasning av glödlampor inom eu. <http://kemi.se/sv/Innehall/Fragor-ikfokus/Kvicksilver-i-lagenergilampor-och-lysrör/>, Hämtad 2012-06-15 kl 13.05, 2011-01-24.
- [14] S. Sholupov, S. Pogarev, V. Ryzhov, N. Mashyanov, and A. Stroganov. Zeeman atomic absorption spectrometer ra-915+ for direct determination of mercury in air and complex matrix samples. *Fuel. Process. Technol*, 85(6-7), 2004. 348-349.
- [15] Sune Svanberg. *Atomic and Molecular Spectroscopy: Basic Aspects and Practical Applications*. Springer-Verlag Berlin Heidelberg, 2nd edition, 1992.

- [16] E.D Thoma, C. Secrest, E. S. Hall, D. Lee Jones, R. C Shores, M. Modrak, R. Hashmonay, and P. Norwood. Measurement of total site mercury emission from a chlor-alkali plant using ultraviolet differential optical absorption spectroscopy and cell room roof-vent monitoring. *Atmospheric Environment*, 43(3), 2009. 753-757.

8 Bibliography

Kvicksilver, Kemikalieinspektionen, <http://www.kemi.se/Content/In-focus/Mercury/Start>, Hämtad 2012-06-15 kl 13.00, 2011-01-21

Nylander.A, Kemikalieinspektionen, *Kvicksilver i lågenergilampor och lysrör*, <http://kemi.se/sv/Innehall/Fragor-i-fokus/Kvicksilver-i-lagenergilampor-och-lysrör/Start>, 2012-06-15 kl 13.05, 2011-01-24

Östman.M, Kemikalieinspektionen, Kvicksilver, <http://kemi.se/sv/Innehall/Fragor-i-fokus/Kvicksilver-i-lagenergilampor-och-lysrör/Start>, Hämtad 2012-06-15 kl 13.05, 2011-01-24

Nylander.A, Kemikalieinspektionen, *Kvicksilver i lågenergilampor och lysrör, Tidtabell för utfasning av glödlampor inom EU*, <http://kemi.se/sv/Innehall/Fragor-i-fokus/Kvicksilver-i-lagenergilampor-och-lysrör/>, Hämtad 2012-06-15 kl 13.05, 2011-01-24

Livsmedelsverket, <http://www.slv.se/sv/grupp1/Risker-med-mat/Metaller/>, Hämtad 2012-06-15 kl 14.02

T.N Anderson, J.K Magnuson and R.P Lucht, *Diode-laser-based sensor for ultraviolet absorption measurements of atomic mercury*, Applied Physics B, 2007

J.Alnis, U.Gustafsson, G.Somesfalean and S.Svanberg, *Sum-frequency generation with a blue diode laser for mercury spectroscopy at 254 nm*, Applied Physics Letters, 76(10), 6 March 2000

Xiutao Lou, G.Somesfalean, S.Svanberg, Zhiguo Zhang and Shaohua Wu, *Detection of elemental mercury by multimode diode laser correlation spectroscopy*, Optics Express, 20(5), 13 Feb 2012

Hans Edner, Gregory W.Faris, Anders Sunesson and Sune Svanberg, *Atmospheric atomic mercury monitoring using differential absorption lidar techniques*, Applied Optics, 28(5), 1 March 1989

X.T.Lou, G.Somesfalean and S.Svanberg, *Sulphur dioxide measurements using an ultraviolet light-emitting diode in combination with gas correlation techniques*, Applied Physics B, 13 February 2009

Feng Xu, She Lv, Xiutao Lou, Yungang Zhang and Zhigou Zhang, *Nitrogen dioxide monitoring using a blue LED*, Applied Optics, 47(29), 10 October 2008

H. Edner, A. Sunesson, S. Svanberg, L. Unéus and S. Wallin, *Differential optical absorption spectroscopy system used for atmospheric mercury monitoring*, Applied Optics, 1986, 25(3), 403-409

E.D Thoma, C. Secrest, E. S. Hall, D. Lee Jones, R. C Shores, M. Modrak, R. Hashmonay and P. Norwood, *Measurement of total site mercury emission from a chlor-alkali plant using ultraviolet differential optical absorption spectroscopy and cell room roof-vent*

monitoring, Atmospheric Environment, 2009, 43(3), 753-757

S. Sholupov, S. Pogarev, V. Ryzhov, N. Mashyanov and A. Stroganov", *Zeeman atomic absorption spectrometer RA-915+ for direct determination of mercury in air and complex matrix samples*, Fuel. Process. Technol, 2004,85(6-7), 348-349

T. Hadeishi, D. A. Church, R. D. McLaughlin, B. D. Zak, M. Nakamura and B. Chang, *Mercury monitor for ambient air* Science, 1975, 187(4147), 348-349

Gilbert Jönsson, *Grundläggande fysik om gaser och vätskor*, 1998, Studentlitteratur. Sweden

Kenneth S Krane, *Introductory nuclear physics*, 1998, John Wiley & Sons.Inc

A.Thorne, U.Litzén and S.Johansson, *Spectrophysics principles and applications*, 2007, Mediatryck

Sune Svanberg, *Atomic and Molecular Spectroscopy: Basic Aspects and Practical Applications*, 2nd, 1992,
Springer-Verlag Berlin Heidelberg

Sharon Ann Holgate, *Understanding Solid State Physics*, 2010, Taylor & Francis Group

J.J Sakurai and Jim Napolitano, *Modern Quantum Mechanics*, 2011, Pearson Education. In publishing as Addison-Wesley

K.F.Riley, M.P.Hobson and S.J.Bence, *Mathematical methods for physics and engineering*, 2007, Cambridge University Press